Agenda Item: 8.1.1.1
Source: National Taiwan University
Title: **Evaluation Results of CPS-OFDM Waveform**
Document for: Discussion and Decision

1 Introduction

In the study item proposal of 5G new radio access technology (RAT) [1], it was agreed that Phase I specification of the new RAT must be forward compatible (in terms of efficient co-cell/site/carrier operation) with Phase II specification and beyond. For the fundamental physical layer signal structure, new radio (NR) waveform is based on OFDM with potential support of non-orthogonal property and multiple access. Fundamental radio frequency (RF) aspects that may impact decisions on the new RAT are required to be considered. Besides, the new RAT is necessary to enable efficient multiplexing of traffic for different services and use cases on the same contiguous block of spectrum.

In RAN1#86 meeting [8], there are several agreements with respect to new waveform development. Here we briefly enumerate the key agreements related to our work:

- At least up to 40 GHz for eMBB and URLLC services, NR supports CP-OFDM based waveform with Y[1] greater than that of LTE (assuming Y=90% for LTE) for DL and UL, possibly with additional low PAPR/CM technique(s) (e.g., DFT-S-OFDM, etc.)
- In-band frequency multiplexing of different numerologies is supported in NR for both DL and UL.
- From RAN1 perspective, spectral confinement techniques for a waveform at the transmitter are transparent to the receiver.
- NR uplink should target at least the same link budget (i.e. MCL) as LTE uplink, under the same usage scenarios and similar deployment configurations (e.g., same carrier frequency).
- When considering DL and UL waveforms for spectrum band above 40GHz, RAN1 should at least consider the impact of low PA efficiency, phase noise, and Doppler impairments.
- RAN1 should continue study whether/how to support guard-band for inter-subband interfering scenarios (e.g., cases 2/3/4) with considerations of the specification/performance impact.

In our related work [2]-[4], CPS-OFDM waveform characterized by precoder flexibility with multiple access support and forward compatibility is proposed to be one of 5G NR waveform candidates. In this document, we provide CPS-OFDM waveform evaluation results according to the parameters given in [5]-[6]. We also show the corresponding performance comparisons with some of waveform candidates proposed in the last two meetings [7]-[8].

1.1 Contributions

This document shows the evaluation results of transmitter complexity, power spectral density (PSD) with power amplifier (PA) nonlinearity agreed in R1-166004, and uncoded bit-error rate (BER) in Case 1a (downlink) and Case 1b (single user in uplink) for CPS-OFDM [3], f-OFDM [9], UF-OFDM [10], W-OFDM [11], WOLA-OFDM [12], and ZT DFT-s-OFDM [13] waveform candidates. Note that both OFDM and DFT-s-OFDM with cyclic prefix (CP) serve as performance references for NR waveform evaluation [7]. In addition, simulation results also demonstrate that CPS-OFDM is much more robust to asynchronous transmissions and mixed numerologies than legacy OFDM and DFT-s-OFDM in Case 2, Case 3, and Case 4.

[1] Y (%) = transmission bandwidth configuration / channel bandwidth $*$ 100%

2 Simulation Setup

Transceiver models of the aforementioned waveform candidates to be evaluated by our simulator are illustrated in block diagram form. The philosophy of notation utilization is in accordance with [3]. The used parameters of DFT-spreading, guard interval, Tx/Rx filtering, and Tx/Rx windowing are also addressed in this section.

2.1 Transceiver Structure

First of all, OFDM and DFT-s-OFDM applied to legacy LTE downlink and uplink are shown in Figure 1 and Figure 2, respectively. At the receiver, benefited from the circulant channel structure, one-tap frequency-domain equalization (FDE) can be used for channel frequency response (CFR) compensation, in zero forcing (ZF) or minimum mean-square error (MMSE) manner. In our all simulations of waveform evaluation, we unify the receiver structure in such way with MMSE-FDE. In addition, it is worthy to note that the utilization of a channel-independent precoder such as DFT-spreading matrix and its corresponding decoder can mitigate the effect of channel spectral nulls so as to improve the detection performance [14].

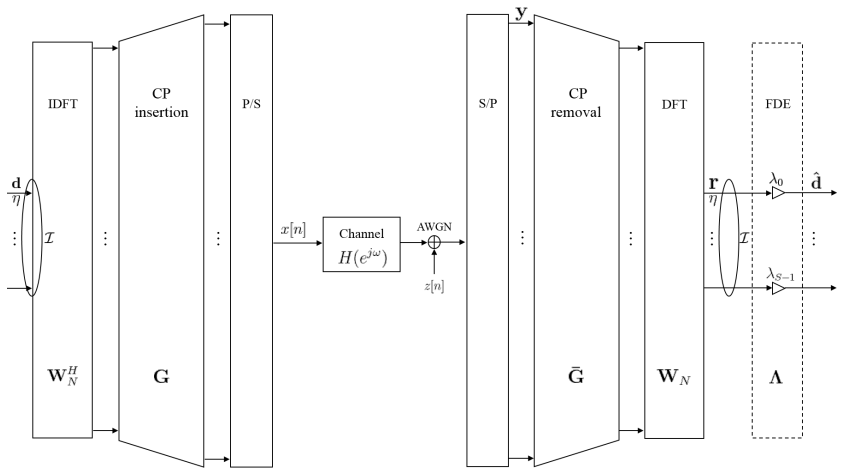

Figure 1: OFDM transceiver.

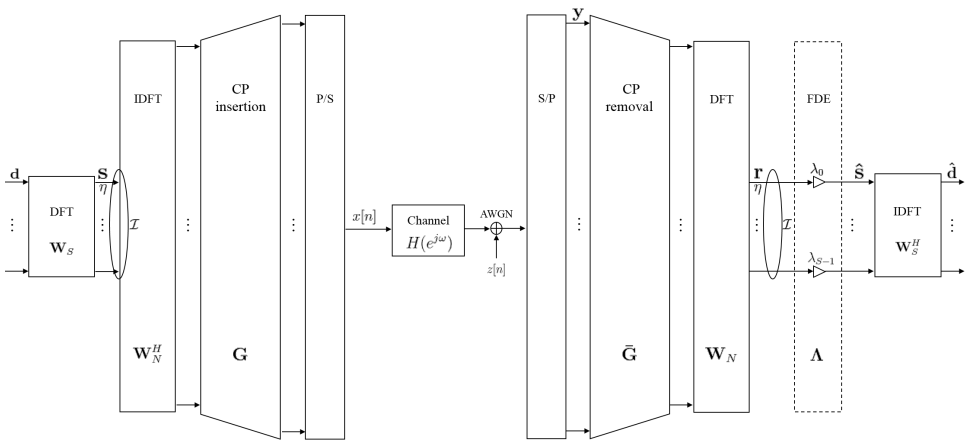

Figure 2: DFT-s-OFDM transceiver.

As stated in [3], CPS-OFDM characterized by the flexibility of its circular pulse shaping percoder can be realized in an efficient way depicted in Figure 3. Here we choose $K = 25$, $M = 24$, $\mathbf{d}_0 = \mathbf{0}_{M\times 1}$, $[\mathbf{d}_k]_0 = 0$, $\forall k$, $Z = 48$, and $\beta = 0$ for single downlink user in Case 1a. For

single uplink user in Case 1b, we choose $K = 3$, $M = 16$, $[\mathbf{d}_k]_0 = 0,\ \forall k$, $Z = 3$, and $\beta = 0.5$. At this stage, for simplicity, raised-cosine coefficients with $\alpha = 0$ and zero padding (ZP) are used for subcarrier-wise shaping and guard interval, respectively. In the future, the shaping coefficients $(\gamma_0, \gamma_1, \cdots, \gamma_{S-1})$ and the intra-subband numerology (depending on the parameters K, M, β, and μ) can be further optimized up to different use cases and requirements.

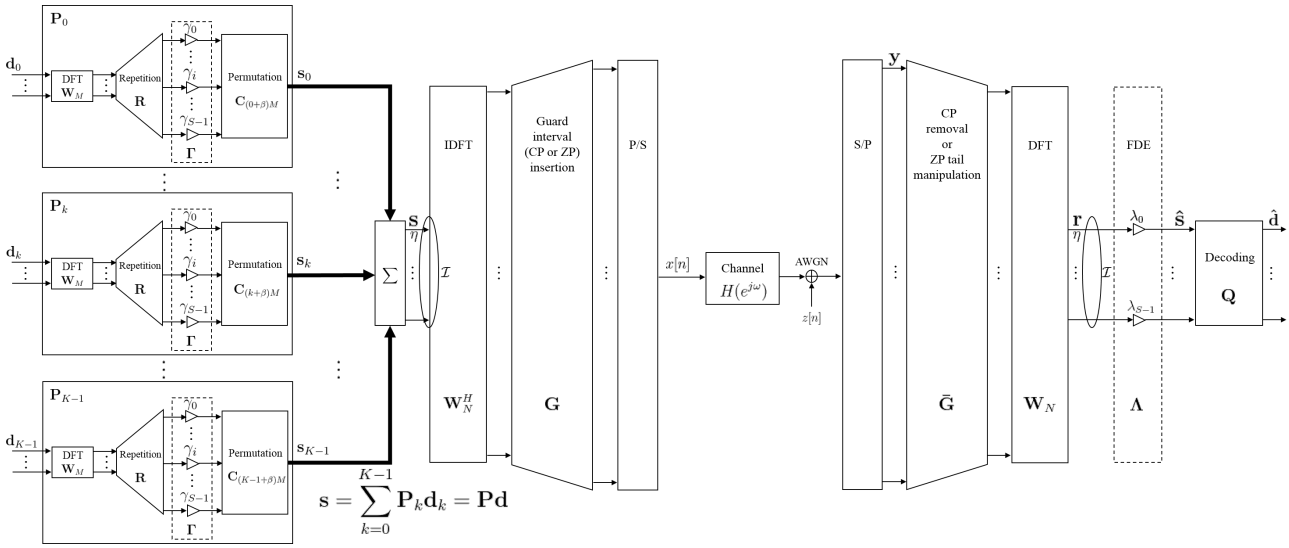

Figure 3: CPS-OFDM transceiver.

To facilitate multiuser downlink (MUDL), multiple CPS precoders are adopted at the transmitter as shown in Figure 4. Unlike UF-OFDM restricted by the Chebyshev filter, different users are able to have different sizes and parameters with respect to their own CPS precoders.

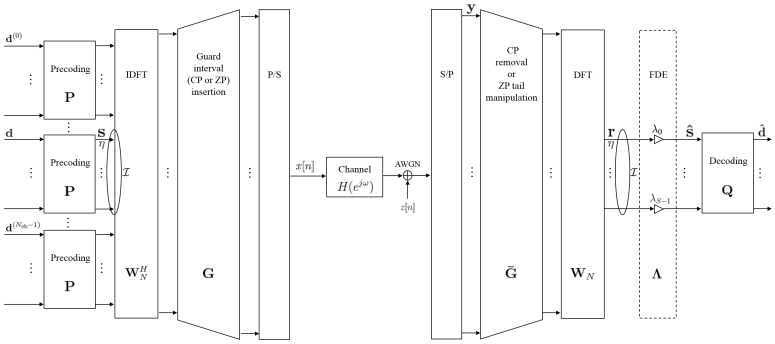

Figure 4: CPS-OFDM transceiver for MUDL.

In Figure 5 and Figure 6, both f-OFDM and UF-OFDM use filtering techniques to suppress out-of-subband (OOSB) emission, but they utilize different filter coefficients and guard intervals. For f-OFDM, the FIR filter $\mathbf{h}_\mathrm{f}$ is generated by imposing the raise-cosine window[2] on the sinc impulse response[3] with tone offset techniques. Two filter orders $L_\mathrm{f} = N/2$ and $L_\mathrm{f} = G$ are taken into account with $N_\mathrm{ToneOffset} = 2.5$ and $N_\mathrm{ToneOffset} = 5$, respectively. For UF-OFDM, the additional precoding matrix is a diagonal matrix whose diagonal entries are to compensate the passband decay caused by the Dolph-Chebyshev filter with the attenuation factor 75 dB and $L_\mathrm{f} = G$. Since the mainlobe of the Chebyshev filter is very narrow, several parallel subband-wise transmissions are required for the wideband scenario of Case 1a as shown in Figure 7. Moreover,

[2] $w[l_\mathrm{f}] = \left(0.5\left(1+\cos\left(\frac{2\pi l_\mathrm{f}}{L_\mathrm{f}}\right)\right)\right)^{0.6}, -\left\lfloor\frac{L_\mathrm{f}+1}{2}\right\rfloor \le l_\mathrm{f} \le \left\lfloor\frac{L_\mathrm{f}+1}{2}\right\rfloor$

[3] $\mathrm{sinc}\left((S+2N_\mathrm{ToneOffset})l_\mathrm{f}/N\right)$

the filter utilization usually results in significant peak-to-average power ratio (PAPR) increase at the transmitter and inter-block interference (IBI) at the receiver. The linear convolution of an FIR filter and a channel impulse response (CIR) can be regarded as an equivalent CIR to be estimated and equalized.

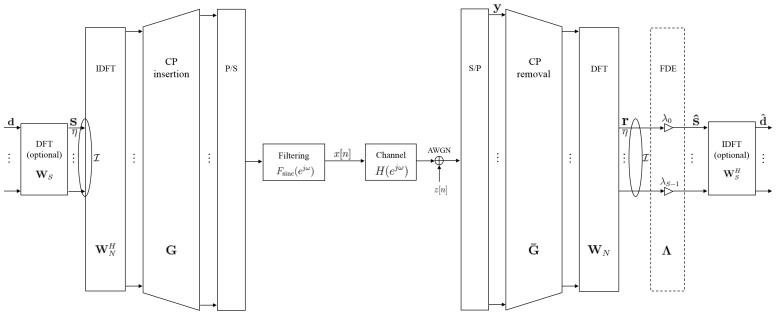

Figure 5: f-OFDM transceiver.

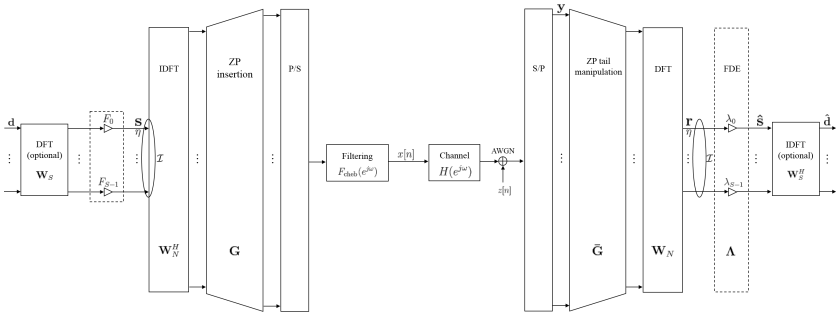

Figure 6: UF-OFDM transceiver.

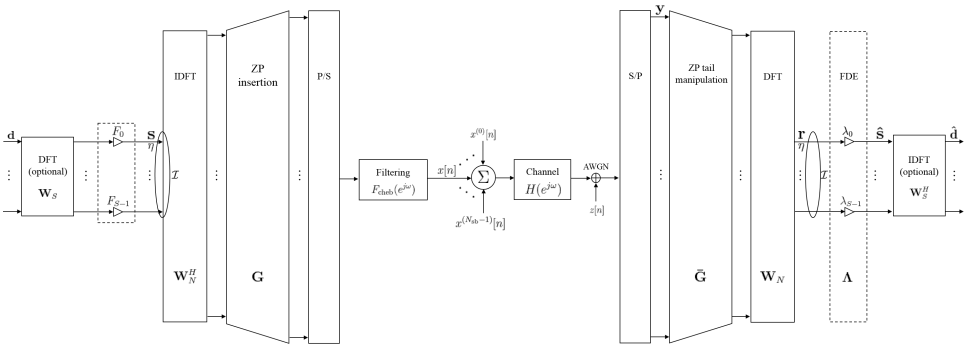

Figure 7: UF-OFDM transceiver for MUDL.

In Figure 8, both W-OFDM and WOLA-OFDM smoothly extend the time-domain block duration by introducing a G-length raised-cosine window to every block edges. The difference is that WOLA-OFDM has an additional block extension in front of CP. Similar to filtering techniques, such windowing techniques leads to IBI impairment. However, they suffer much less distortion of OOSB emission due to PA nonlinearity. In the complexity aspect, the number of multiplications is G, which is much less than that of performing a linear convolution for filtering.

In the simulations of Case 1b for single user uplink scenario, due to PAPR considerations, we adopt DFT-spreading pecoder for f-OFDM, UF-OFDM, W-OFDM, and WOLA-OFDM as shown in Figure 5, Figure 6, and Figure 8.

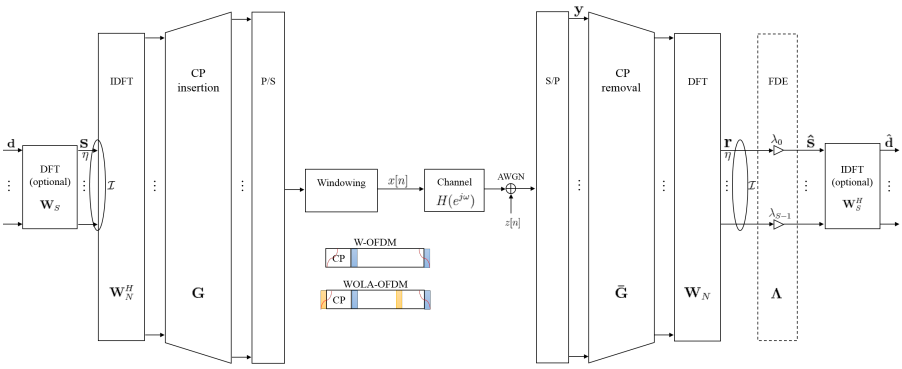

Figure 8: W-OFDM/WOLA-OFDM transceiver

Figure 9 displays the zero-tail (ZT) DFT-s-OFDM transceiver in which guard interval insertion is not needed. We assign the indices of null symbols as $\{0, 1, \cdots, 19, S-27, \cdots, S-1, S\}$ and $\{0, S-1, S\}$ for Case 1a and Case 1b, respectively. Although the power of every block tail is small, IBI always exists because of the lack of guard intervals.

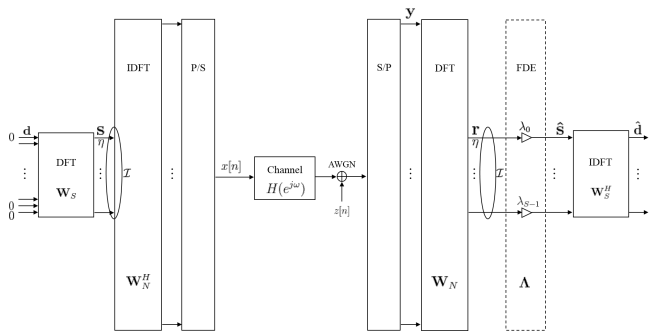

Figure 9: ZT DFT-s-OFDM transceiver.

2.2 System Parameters

Practical system parameters are chosen according to the agreements in the 3GPP RAN1 meeting [5]-[6] as listed in Table 1. At the receiver, the processes of synchronization and channel estimation are assumed to be perfect.

3 Performance Evaluation in Case 1a

The evaluation results of transmitter complexity, PSD with PA nonlinearity, and uncoded BER in Case 1a are provided in this section.

3.1 Transmitter Complexity

The transmitter complexity is evaluated by computing its number of complex multiplications. OFDM, f-OFDM, W-OFDM, and WOLA-OFDM naturally support MUDL. On the other hand, CPS-OFDM, UF-OFDM, and ZT-DFT-s-OFDM are required to be actualized in subband-wise ways. Table 2 summarizes the required number of complex multiplications for the waveform candidates. Here the notations S' ($= K'M'$ for CPS-OFDM) and N_{sb} denote the number of OFDM subcarriers (e.g., $S' = 48$) in each subband and the number of allocated subbands, respectively. Although there exists fast frequency implementation methods to perform filtering,

Table 1: Link-level simulation parameters.

Parameter	**Notation**	**Value**
Carrier frequency		4 GHz
Sampling rate		15.36 MHz
OFDM subcarrier spacing		15kHz
FFT size	N	1024
Guard interval length	G	72
Number of allocated subcarriers	S	600 (for Case 1a); 48 (for Case 1b)
Starting subcarrier index	η	212
Transmission time interval	TTI	1 ms
Modulation scheme		16QAM
Coding scheme		None
Number of antennas		1T1R
Multipath channel model		ETU and TDL-C300 for 3 km/hr
Channel equalization		MMSE-FDE
PA model (agreed in R1-166004)		Rapp (for Case 1a); Polynomial (for Case 1b)
PA operating point	OPP	-12 dBm (for Case 1a); -8 dBm (for Case 1b)

Table 2: Transmitter complexity comparisons.

	Precoder	**IFFT**	**Filter/Window**
OFDM		$N \log_2 N$	
CPS-OFDM	$S(K + \log_2 M)$	$N \log_2 N$	
CPS-OFDM (MUDL)	$N_{\text{sb}} S'(K' + \log_2 M')$	$N \log_2 N$	
f-OFDM		$N \log_2 N$	$N(L_{\text{f}} + 1)$
UF-OFDM (MUDL)	$N_{\text{sb}} S$	$N_{\text{sb}} N \log_2 N$	$N_{\text{sb}} N(L_{\text{f}} + 1)$
W-OFDM		$N \log_2 N$	G
WOLA-OFDM		$N \log_2 N$	G
ZT-DFT-s-OFDM	$S \log_2 S$	$N \log_2 N$	
ZT-DFT-s-OFDM (MUDL)	$N_{\text{sb}} S' \log_2 S'$	$N \log_2 N$	

f-OFDM and UF-OFDM still require much more multiplier units (increasing in the order of N) than others.

3.2 PSD with PA Nonlinearity

In [15], it is proposed that the expected low out-of-band emission (OOBE) obtained by filtering techniques (such as f-OFDM and UF-OFDM) is not achievable when PA nonlinearity is considered. However, CPS-OFDM based on the precoding technique enjoys a much less deterioration in lowering our-of-band (OOB) emission. The simulation results are given in Figure 10 and Figure 11.

Observed from the PSD evaluation results, we find that f-OFDM with $L_{\text{f}} = N/2$ is difficult to meet ACLR threshold when PA nonlinearity is considered. Besides, ZT DFT-s-OFDM cannot meet the ACLR unless using more mull symbols at the cost of spectral efficiency. In Figure 11 (b), we say that the PSD of UF-OFDM is ideal, because we have not considered the required guard subcarriers between any two subbands yet.

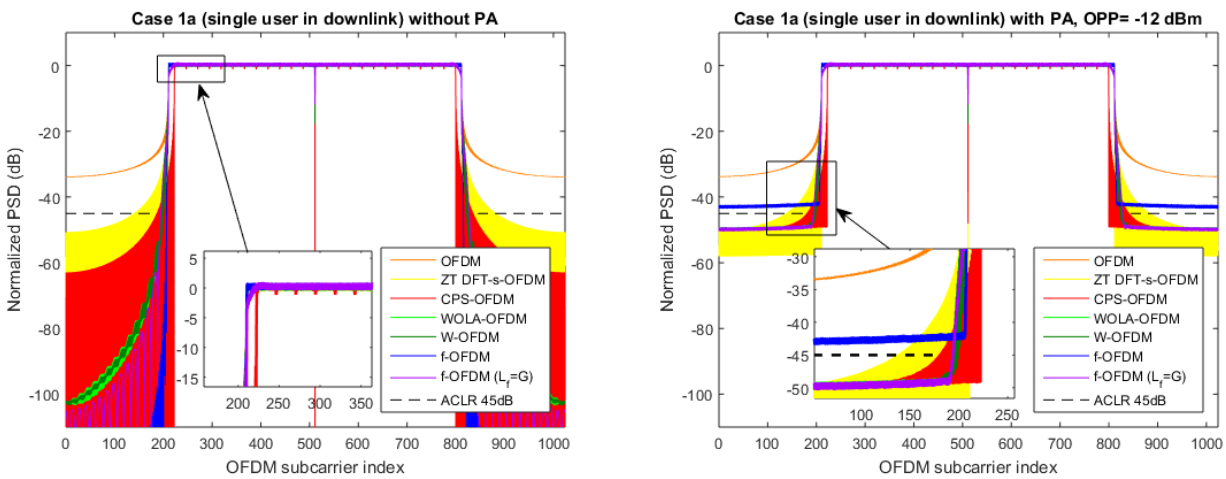

(a) (b)

Figure 10: PSD comparisons (a)without PA, (b) with PA nonlinearity.

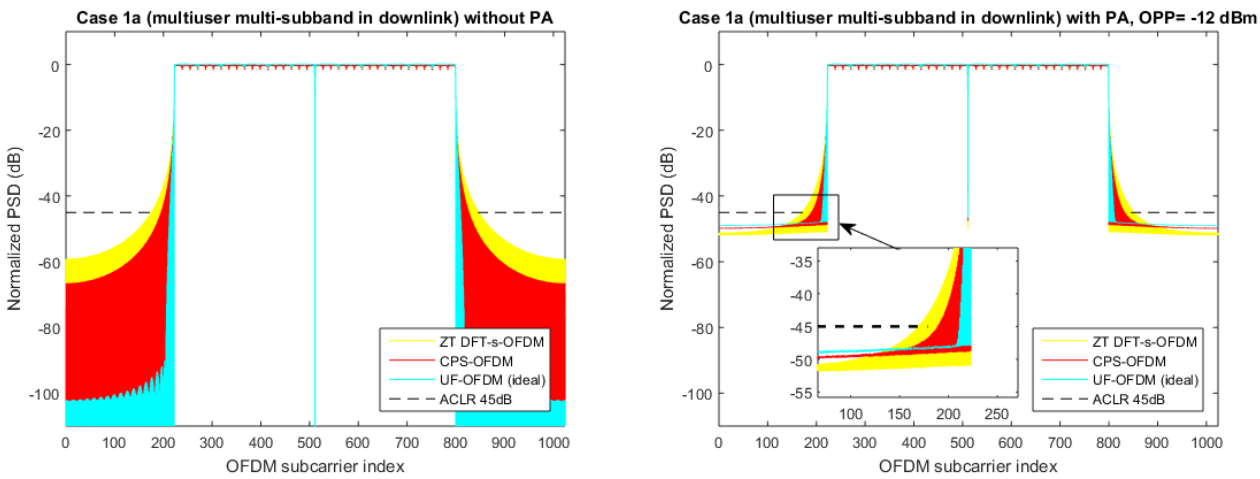

(a) (b)

Figure 11: PSD comparisons for MUDL of CPS-OFDM, UF-OFDM, and ZT DFT-s-OFDM (a)without PA, (b) with PA nonlinearity.

3.3 BER Performance

To know the inherent waveform characterizations, coding schemes and radio frequency (RF) impairments are not considered in our simulations. Since W-OFDM and WOLA-OFDM have similar OOBE performance, we only do the BER evaluation of W-OFDM. Figure 12 shows the BER evaluation results for single downlink user wideband scenario in ETU and TDL-C-300 channel environments. Among these new waveform candidates, only CPS-OFDM simultaneously guarantees IBI-free reception and low OOB/OOSB emission.

4 Performance Evaluation in Case 1b

The evaluation results of transmitter complexity, PSD with PA nonlinearity, and uncoded BER in Case 1b are provided in this section.

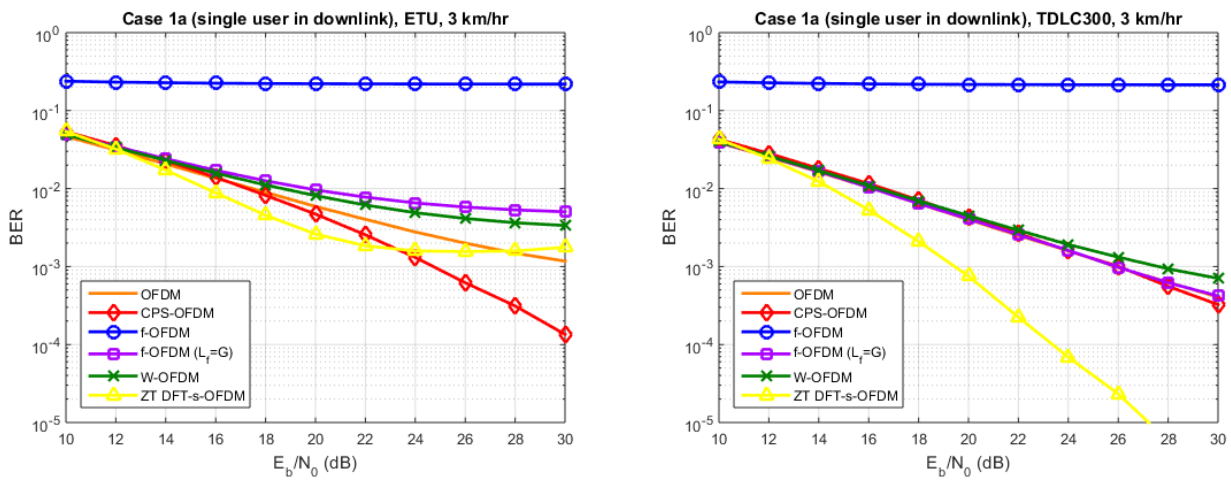

(a) (b)

Figure 12: BER comparisons (a) ETU channel, (b) TDL-C-300 channel.

4.1 Transmitter Complexity

Table 3 summarizes the required number of complex multiplications for the waveform candidates. Compared to the utilization of an S-point DFT precoder, the proposed CPS precoder slightly increases the complexity by $KM(K - \log_2 K)$ complex multiplications, $S = KM$. Note that the repetition and the permutation operations can be actualized without multiplier units.

Table 3: Transmitter complexity comparisons.

	Precoder	**IFFT**	**Filter/Window**
DFT-s-OFDM	$S \log_2 S$	$N \log_2 N$	
CPS-OFDM	$S(K + \log_2 M)$	$N \log_2 N$	
f-OFDM	$S \log_2 S$	$N \log_2 N$	$N(L_\mathrm{f} + 1)$
UF-OFDM	$S(\log_2 S + 1)$	$N \log_2 N$	$N(L_\mathrm{f} + 1)$
W-OFDM	$S \log_2 S$	$N \log_2 N$	G
WOLA-OFDM	$S \log_2 S$	$N \log_2 N$	G
ZT-DFT-s-OFDM	$S \log_2 S$	$N \log_2 N$	

4.2 PSD with PA Nonlinearity

It is important to consider PA nonlinearity especially for future 5G low-cost machines (e.g., sensors). Figure 13 shows the PSD evaluation results for single uplink user transmission.

Observed from the simulation results, the low OOSB emission properties of f-OFDM and UF-OFDM greatly degraded when the effect of PA nonlinearity is considered, as predicted by [15]. As a contrast, CPS-OFDM suffers much less OOSB emission performance degradation. The main reason behind this is that CPS-OFDM has a much lower PAPR than f-OFDM and UF-OFDM [3].

4.3 BER Performance

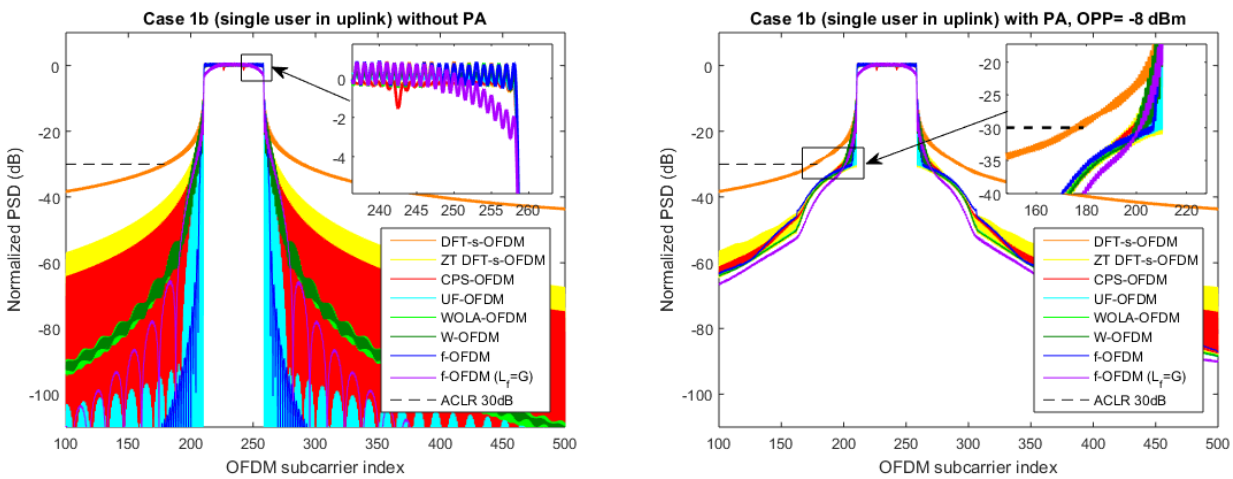

(a) (b)

Figure 13: PSD comparisons (a)without PA, (b) with PA nonlinearity.

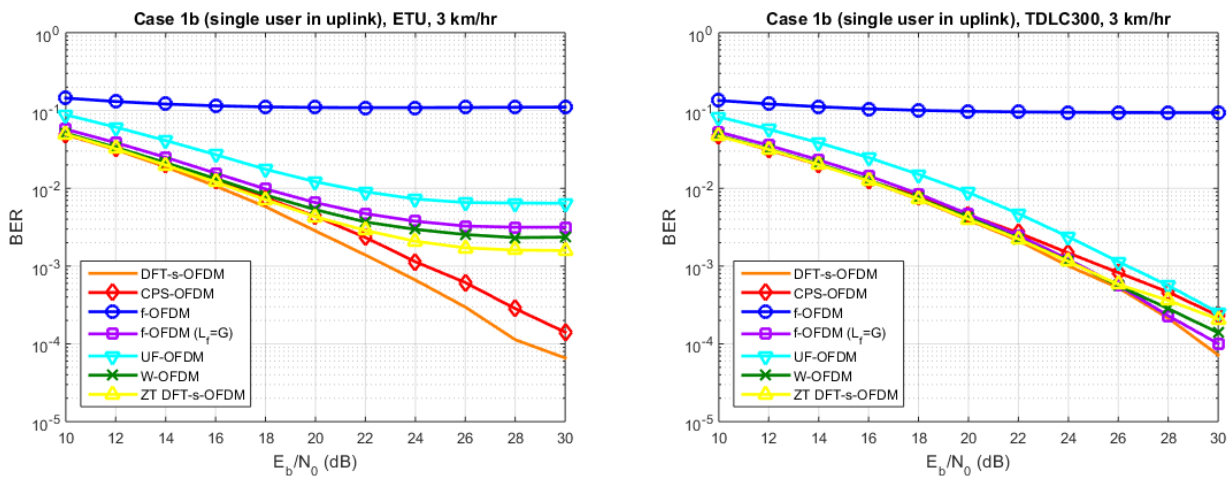

(a) (b)

Figure 14: BER comparisons (a) ETU channel, (b) TDL-C-300 channel.

5 Performance Evaluation in Case 2/3/4

Simulation parameters are chosen according to the agreements in the 3GPP RAN1 meeting [5]-[6]. Basic system parameters are listed in Table 4. The performance metric is uncoded bit-error rate (BER) measured by the target receiver. The parameters of the target user for evaluation are shown in Table 5.

Case 2 is a downlink scenario in which the target user equipment (UE) is interfered by the adjacent subband transmission using 30 kHz subcarrier spacing.

Here we simplify Case 3 to be a "two-user" asynchronous uplink scenario with the same numerology, in which the signal of the interfering UE arrived at the base station (BS) is delayed by $\{0, 128, 512\}$ timing offset samples.

Case 4 is also simplified to be a "two-user" uplink scenario with mixed numerologies, where the transmission of the target UE and the interfering UE are based on 15 kHz and $\{30, 15, 7.5\}$ kHz subcarrier spacing values, respectively.

Table 4: System parameters.

Parameter	**Value**
Carrier frequency	4 GHz
Sampling rate	15.36 MHz
Guard interval overhead	6.7%
Data transmission bandwidth per user	720 kHz
Number of users	2
Power offset of the interfering user	0 dB
Bandwidth of guard tones between the two users	60 kHz
Modulation scheme	16QAM
Coding scheme	None
Number of antennas	1T1R
Multipath channel model	TDL-C-300 for 3 km/hr
Channel equalization	MMSE-FDE

Table 5: Target user parameters.

Parameter	**Notation**	**Value**
Subcarrier spacing		15 kHz
Number of allocated subcarriers	S	48
FFT size	N	1024
Number of timing offset samples	τ	0

5.1 BER Performance Evaluation

The uncoded BER evaluation results in Case 2, Case 3, and Case 4 are presented in this subsection.

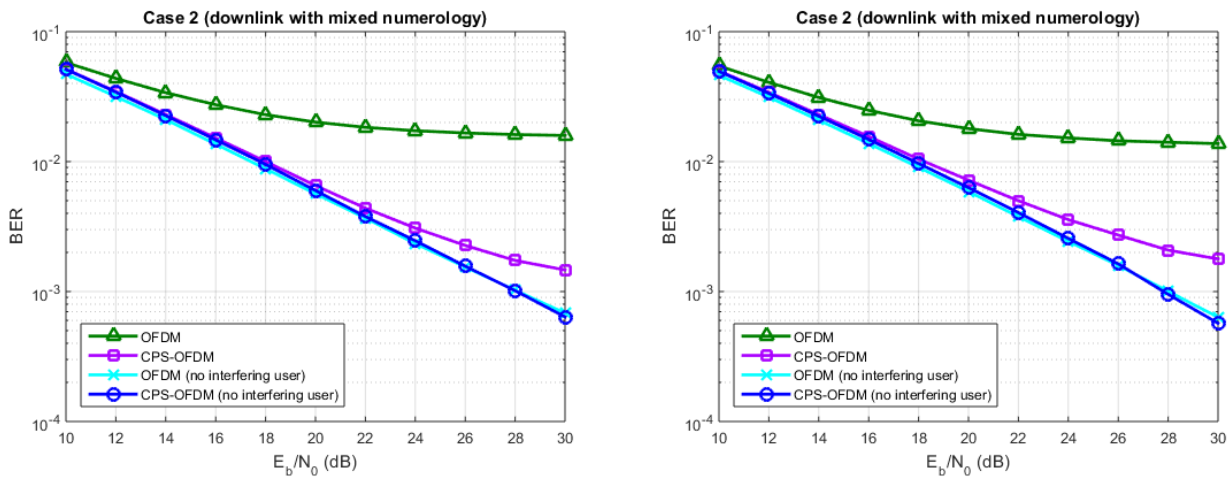

(a) (b)

Figure 15: Robustness of CPS-OFDM to multiuser downlink with mixed numerologies (a) without PA, (B) with PA nonlinearity.

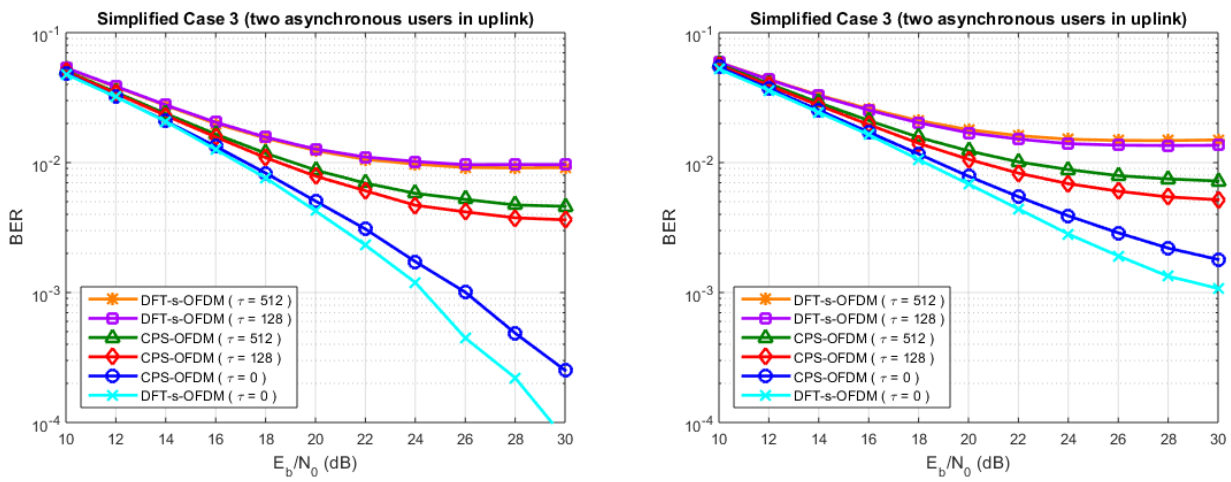

(a) (b)

Figure 16: Robustness of CPS-OFDM to multiuser uplink with timing offset (a) without PA, (B) with PA nonlinearity.

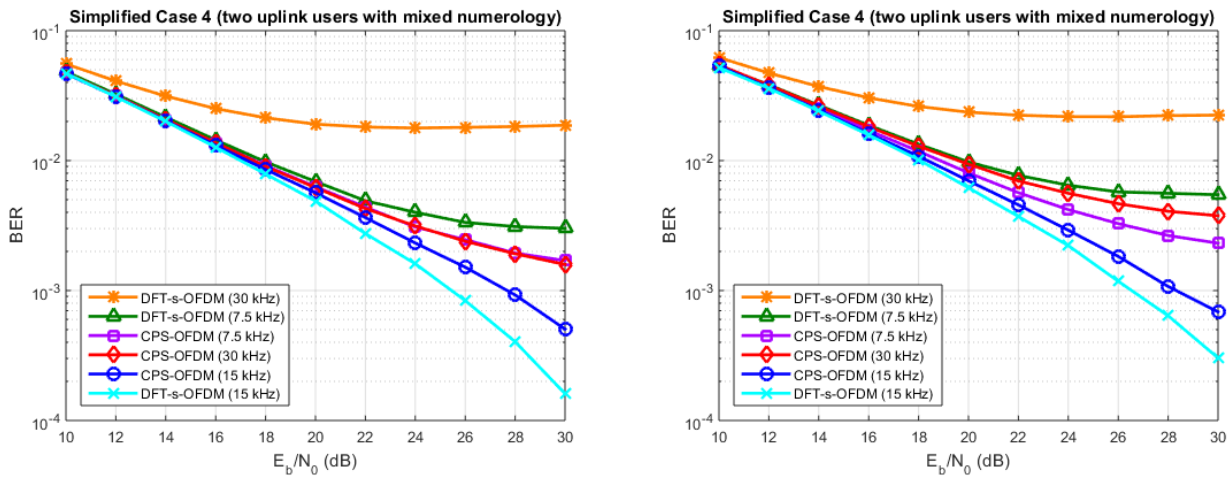

(a) (b)

Figure 17: Robustness of CPS-OFDM to multiuser uplink with mixed numerologies (a) without PA, (B) with PA nonlinearity.

6 Summary

CPS-OFDM waveform characterized by precoder flexibility with multiple access support and forward compatibility is designed to facilitate 5G fragmented spectrum usage. Based on the evaluation results, we summarize the observations and then make one proposal as follows:

Observation 1: *CPS-OFDM is efficient in transmitter implementation and flexible in determining desired transmission properties for each user.*

Observation 2: *CPS-OFDM enjoys a much less deterioration in lowering OOB/OOSB emission compared to f-OFDM and UF-OFDM when the effect of PA nonlinearity is considered.*

Observation 3: *Unlike most of NR waveform candidates, CPS-OFDM prevents detection performance degradation due to IBI.*

Observation 4: *CPS-OFDM is much more robust to asynchronous transmissions and mixed numerologies than legacy OFDM and DFT-s-OFDM.*

Proposal 1: *Consider the advantages of IBI-free reception, low OOB/OOSB emission with PA nonlinearity, low-complexity transceiver implementation, multiple access support, backward/forward compatibility, and robustness to asynchronous transmissions and mixed numerologies, CPS-OFDM can be one of highly-potential waveforms in NR.*

References

[1] NTT DOCOMO, "New SID proposal: study on new radio access technology," 3GPP RAN #71 Meeting, Technical Document RP-160351, Gothenburg, Sweden, March 7-10, 2016.

[2] National Taiwan University, "Precoder flexibility and forward compatibility of CPS-OFDM waveform," 3GPP RAN1 #86bis Meeting, Technical Document R1-1610107, Lisbon, Portugal, Oct. 10-14, 2016.

[3] National Taiwan University, "Fundamentals of CPS-OFDM waveform for 5G new radio," 3GPP RAN1 #86 Meeting, Technical Document R1-167820, Gothenburg, Sweden, Aug. 22-26, 2016.

[4] National Taiwan University, "OFDM-based waveform with precoding techniques," 3GPP RAN1 #85 Meeting, Technical Document R1-165113, Nanjing, China, May 23-27, 2016.

[5] Huawei and HiSilicon, "Way forward on assumptions for waveform evaluation," 3GPP RAN1 #84bis Meeting, Technical Document R1-163558, Busan, Korea, Apr. 11-15, 2016.

[6] Huawei, HiSilicon, NTT DOCOMO, and Nokia, "Way forward on calibration assumptions for NR waveform," 3GPP RAN1 #85 Meeting, Technical Document R1-165989, Nanjing, China, May 23-27, 2016.

[7] 3GPP, "RAN1 chairman's notes," New Radio (NR) in RAN1#85 meeting, Nanjing, China, May 23-27, 2016.

[8] 3GPP, "RAN1 chairman's notes," New Radio (NR) in RAN1#86 meeting, Gothenburg, Sweden, Aug. 22-26, 2016.

[9] Huawei and HiSilicon, "f-OFDM scheme and filter design," 3GPP RAN1 #85 Meeting, Technical Document R1-165425, Nanjing, China, May 23-27, 2016.

[10] Nokia and Alcatel-Lucent Shanghai Bell, "Subband-wise filtered OFDM for new radio below 6 GHz," 3GPP RAN1 #85 Meeting, Technical Document R1-165014, Nanjing, China, May 23-27, 2016.

[11] Ericsson, "Feasibility of mixing numerology in an OFDM system," 3GPP RAN1 #84bis Meeting, Technical Document R1-163224, Busan, Korea, Apr. 11-15, 2016.

[12] Qualcomm Inc., "OFDM based waveform single user evaluation," 3GPP RAN1 #85 Meeting, Technical Document R1-164685, Nanjing, China, May 23-27, 2016.

[13] G. Berardinelli and et al., "On the potential of OFDM enhancements as 5G waveforms," in *Proc. IEEE 79th Vehicular Technology Conference (VTC Spring)*, May 2014.

[14] Y. -P. Lin and S. -M. Phoong, "BER minimized OFDM systems with channel independent precoders," *IEEE Trans. on Signal Processing*, vol. 51, no. 9, pp. 2369-2380, Sep. 2003.

[15] Skyworks Solutions Inc., "NR candidate waveforms: UL performance issues for PAPR, out-of-channel emissions, and RF front-end linearity/efficiency,," 3GPP RAN1 #85 Meeting, Technical Document R1-165035, Nanjing, China, May 23-27, 2016.